Beamforming Oriented Topology Control for mmWave Networks

Prosanta Paul, Hongyi Wu, ChunSheng Xin, and Min Song

Abstract—The *millimeter wave* (mmWave) frequency band is a promising candidate for next generation cellular and wireless networks. To compensate the significantly higher path loss due to the higher frequency, the mmWave band usually uses the beamforming technology. However, this makes the network topology control a great challenge. In this paper, we propose a novel framework for network topology control in mmWave networks, termed *Beamforming Oriented tOpology coNtrol* (BOON). The objective is to reduce total transmit power of base stations and interference between beams. BOON smartly groups nearby user equipment into clusters, constructs sets from user equipment clusters, and associates user equipment to base stations and beams. We compare BOON with three existing topology control schemes in terms of transmit power, network sum rate, signal to interference and noise ratio, and computation complexity. The results indicate that overall BOON significantly outperforms them. In particular, on average BOON uses only 10%, 32%, and 25% transmit power of other three schemes, respectively, to achieve the same network sum rate.

Index Terms—mmWave networks, topology control, clustering, set covering.

1 Introduction

In recent years we have witnessed remarkable proliferation of intelligent wireless devices. For instance, by the Internet of Things (IoT) forecast of Ericsson, there will be 29 billion IoT devices by 2022 [1]. At the same time, mobile broadband services such as HD video streaming and virtual/augmented reality will continue driving the demand for higher data rates. Such phenomenal growth demands significant higher wireless system capacity. To dramatically increase system capacity, more spectrum needs to be pressed into service. This is because while the wireless spectrum efficiency has improved continuously, such advances cannot meet the requirement for drastic growth in wireless capacity. Today's wireless systems mainly operate in the sub-6 GHz microwave spectrum, which is experiencing severe shortage and has become a precious resource. To this end, the *millimeter wave* (mmWave) band, operating at frequencies between 20 and 300 GHz, has been identified as a promising candidate for next generation cellular systems (5G) and WiFi networks (IEEE 802.11ad) [2]–[7]. The massively underutilized spectrum at the mmWave band provides a great potential to support user data rates of multi-gigabit per second and a thousand-fold increase in system capacity.

While the use of mmWave band addresses the strong demand for wireless spectrum, it brings new technical challenges. The much higher frequency of the mmWave band results in about $20 - 25$ dB higher path loss than today's cellular bands [3], [4]. To overcome this problem, beamforming is adopted where an antenna array is used to generate sharp beams to achieve high signal gain at receivers, by controlling the amplitudes and phases of the signals transmitted (or received) at each element. While it can significantly increase the reach of *base stations* (BSs), beamforming raises a great challenge to form topology in mmWave networks, in particular for multi-BS mmWave networks. This is because we have to design beams to cover all *user equipment* (UE) while avoiding strong interference to each UE from other beams of the same BS or different BSs. This results in a joint beamforming optimization problem among BSs, including UE association among BSs and inter-beam and inter-BS interference reduction. This problem is fundamentally challenging. Without a careful design, the system performance such as the sum rate can be poor while consuming significant resource such as transmit power.

In this paper, *topology control* is referred to as a framework of *user equipment* (UE) association, discovery of the number of beams for each BS and UE coverage by each beam, and multi-BS beamforming in a mmWave network. In traditional cellular networks, the omnidirectional antenna is used and the coverage of a BS is a circular area (cell) based on the communication range of the BS. The topology control is thus straightforward, since it is easy to determine the preferred BS for a UE as well as the preferred UEs for a BS. Unlike traditional cellular networks, a cell or the coverage area of a BS in mmWave networks is complicated and usually has an irregular shape. The coverage area of a BS is essentially the area covered by the beams formed by the BS. The network connection between a BS and a UE relies on whether there is a beam from the BS to cover the UE, rather than the distance between them. On the other hand, where and how to form beams depend on a number of factors such as the UE spatial distribution, interference between beams, power budget, etc. Hence, topology control in mmWave networks is fundamentally challenging.

A straightforward approach to form network topology for mmWave networks is to construct a beam to each UE through *multi-user beamforming* (MUB) [8], [9]. However,

- *P. Paul, H. Wu, and C. Xin are with the Department of Electrical and Computer Engineering, Old Dominion University, Norfolk, VA, 23529. E-mail: {ppaul001, h1wu, cxin}@odu.edu.*
- *M. Song is with the ECE Department, Stevens Institute of Technology, Hoboken, NJ 07030, Email: Min.Song@stevens.edu.*

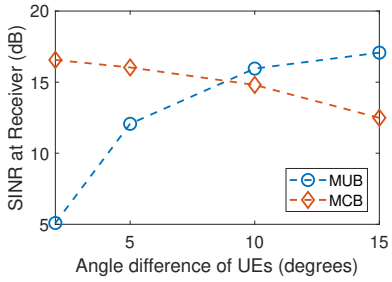

Fig. 1. Average SINR of two UEs as a function of their angular separation relative to the BS

forming one beam for each UE can result in significant interference between nearby UEs, thus degrading system performance such as the *signal to interference and noise ratio* (SINR) at the UEs. Furthermore, each beam needs a *radio frequency* (RF) chain or *beamformer*, which is prohibitively costly or impossible in large scale mmWave networks. Another straightforward approach for topology control is to construct one beam to cover all UEs associated with a BS, through *multicast beamforming* (MCB) [10]–[12]. However, this approach cannot form sharp beams, resulting in wasteful energy consumption. Fig. 1 illustrates the average SINR of two UEs of a BS as a function of their separation angle under MUB and MCB. The transmit power is 4 watt, the UE-BS distance is 100 meters, and the number of antenna elements is 16. Clearly, for MUB, a large separation angle results in a good SINR, while a small separation angle results in a poor SINR, due to the strong interference between the two beams. In contrast, for MCB, a small separation angle results in a good SINR, while a large separation angle results in a poor SINR, because beams are not formed to concentrate power on UEs.

In this paper, we propose a framework for topology control in mmWave networks, termed *Beamforming Oriented tOpology coNtrol* (BOON), to combine the benefits of MUB and MCB based topology control approaches. BOON smartly clusters UEs into groups and form beams based on the groups. Thus, nearby UEs are covered using the same beam to avoid interference, while UEs sufficiently separated, i.e., from different groups, are covered by different beams, to avoid wasteful energy consumption. Furthermore, BOON smartly associates UEs to different BSs and beams, and finds appropriate beamforming vectors for all BSs and beams, with the objective to reduce the interference between BSs and beams. The objective of BOON is to reduce the total transmit power. BOON can significantly reduce mutual interference between nearby UEs and between BSs, resulting in lower power consumption, and reduce system cost by using significantly fewer beams, compared with the MUB based topology control. On the other hand, it can form sharp beams to focus energy on the UEs to reduce power consumption, compared with the MCB based topology control.

There have been several studies on topology control or UE selection in MIMO systems in the literature. In [8], the authors proposed a UE selection method based on channel orthogonality between different UEs, to select a group of UEs with orthogonal channel vectors, which are then served using the MUB scheme. In [9], the authors proposed a user selection scheme to maximize the harmonic sum of UE SINR, which prioritizes cell-edge users to increase throughput, where a UE can receive multiple spatial streams from different BSs. In [13], UEs are partitioned into UE groups, with each group having similar channel covariances. All UEs in a group are served simultaneously using one precoding vector through an MCB scheme. In [14], the authors studied a simpler beamforming scheme called switched beamforming. In [15]–[18], the UEs with uncorrelated or orthogonal channels are grouped together, and then served using the MUB scheme. In [19], [20], a BS forms a beam in a random direction, which can cover UEs in that direction. Most of those works focused on beamforming with one BS, while the UE association among multiple BSs assumed a simple scheme based on the strongest received signal power. In this paper, we not only consider UE selection for a single BS, but also aim to optimize UE association among BSs, with the objective to reduce interference between beams of different BSs.

Our contributions are summarized below.

- We develop a beamforming oriented UE clustering algorithm to group UEs, with the objective to reduce transmit power and interference between beams.
- We devise a set construction scheme and an interference aware set covering algorithm that addresses the unique challenges in beamforming to smartly associate UEs to beams and BSs, with the objective to reduce interference between beams.
- We design an approach to form beams for all BSs with the objective to reduce the total transmit power and inter-BS interference, subject to coverage of all UEs and meeting a minimum quality of service.

The rest of the paper is organized as follows. Section 2 presents an overview of BOON. Section 3 describes the system model. The BOON framework is presented in Section 4. Section 5 presents performance evaluation. Section 6 concludes the paper and discusses future directions.

2 BOON Overview

BSs are deployed by wireless operators and are generally connected to a cloud or a backend management system, through either wired or wireless backhaul connections. Hence, the BSs information, including locations, the number of antennas, etc., is known to the network operator. We assume a low mobility UE network where the updating of UE locations at the BS or the cloud can be at the order of seconds. For a walking speed mobile UE, the channel fading characteristics remain unchanged for several seconds [13], [14]. This means UE tracking can be done at a slow rate. The message exchange delay is expected to be small, e.g., in the order of 1 millisecond in 5G networks. In a low mobility network, the BOON algorithm can be re-run at a frequency in the order of seconds. Both the message exchange delay and running time of BOON are acceptable compared with such an interval. On the other hand, mmWave networks are not well suited for high mobility UE networks [13]. This is because the Doppler shift in wireless channels increases linearly with the carrier frequency and UE mobility, and

the expected angular spread of UE signals at the BS is also higher in mmWave frequency [6], [13].

In general, there are two approaches for a BS to discover UEs. The first approach is to utilize *beam sweeping* [21], [22]. Each BS transmits initial signals in random directions to sweep the whole angular space, to discover UEs. This approach has a lower system cost, but may result in a large delay. The second approach utilizes co-existing macrocells for UE discovery, e.g., LTE towers, to achieve low delay [23]. Given that major cellular operators all have deployed LTE systems, this approach is a feasible solution. Both LTE towers and mmWave BSs are connected to a cloud. The mmWave system off-loads data transport, while the LTE system is used for control and data transport for UEs that cannot be covered by mmWave BSs. The discovery of UE locations results in some overhead. Nevertheless, this overhead is not significant, as the message exchange between LTE towers and UEs is fast.

Through UE discovery, the UEs information, including locations, the *angle of arrival* (AoA) of UE signals, etc., is also known to the mmWave network operator. BOON resides in the cloud of the operator to coordinate topology control among BSs and UEs. It finds the optimal number of beams for each BS, assigns UEs to be covered by each beam, and computes the beamforming vectors for all beams. The objective is to reduce the total transmit power and interference between beams and between BSs, while covering all UEs and meeting a minimum quality of service. As illustrated in Fig. 2, there are four components in BOON: 1) *beamforming oriented UE clustering* (BOC), 2) *cluster decomposition based set construction* (CDSC), 3) *interference aware set covering* (IASC), and 4) *multi-BS beamforming*. BOC carries out fine granularity UE clustering for each BS among all UEs that can be reached through beamforming by the BS. Both the angles of UEs relative to the BS and the distance between UEs are considered in the clustering similarity metric. CDSC decomposes each cluster formed by BOC into a list of overlapping sets, which can be viewed as a list of overlapping sectors, starting from a BS outward. IASC addresses the unique challenges in beamforming and solves a *weighted set covering* problem to select a list of sets among all sets constructed by CDSC, to jointly cover all UEs, with the objective to reduce interference between beams and between BSs. The resulted sets from IASC determine the UE association and BS beam coverage. At last, one beam is formed for each set selected by IASC, with the objective to reduce the total transmit power of all BSs. The BOC algorithm can be run either distributedly at each BS, or at the cloud. The CDSC, IASC, and beamforming can be centrally run at the cloud. However, they can also be implemented in a distributed mode by exchanging the UE clustering information between BSs.

3 System Model

In this section, we describe the system model for BOON, including mmWave channel modeling, transmit power computation, and UE downlink data rate computation. Table 1 lists major notations used in this section.

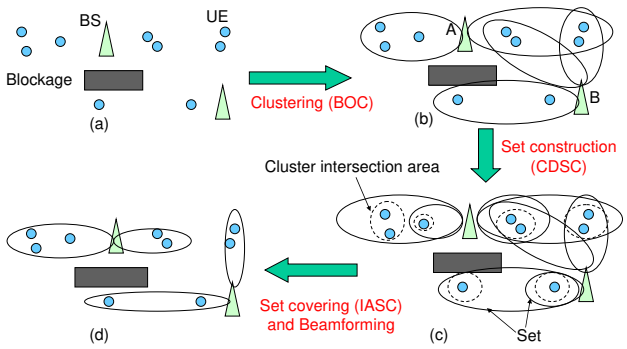

Fig. 2. BOON: (a) UE clustering through the BOC algorithm, (b) set construction (CDSC), (c) set covering to optimally select UE-BS association and select sets for beamforming through the IASC algorithm, (d) beamforming for all BSs based on the selected sets.

TABLE 1
Major notations

m, n, k	index for BS, UE and beam, respectively
$B, \mathcal{U}, C, \mathcal{B}$	set of BSs, UEs, beams, and UE-clusters, respectively
$\langle m, k \rangle$	the k-th beam of the m-th BS
$\theta_{mn}, \mathbf{a}_{\theta_{mn}}$	angle of arrival of UE n signal at BS m array and the corresponding steering vector, respectively
$\mathbf{h}_{mn}$	channel gain vector between BS m and UE n
$\mathbf{w}_{mk}$	beamforming weight vector of beam $\langle m, k \rangle$
ϕ^{hp}_{mk}	half power beamwidth of beam $\langle m, k \rangle$
p^t_{mk}	transmit power of beam $\langle m, k \rangle$
$p^r_{n,m,k}$	received power at UE n from beam $\langle m, k \rangle$
K	maximum number of beamformers at a BS
$I_{n,m,k}, r_{n,m,k}, \gamma_{n,m,k}$	interference, rate, and SINR at UE n when it is served by beam $\langle m, k \rangle$
γ_o	minimum required SINR for UEs

3.1 mmWave Channel

Let $\mathcal{U}$, B and C_m be the set of UEs, BSs, and beams of BS m ($m \in B$), respectively. Let $\mathcal{U}_m \subset \mathcal{U}$ be the set of UEs that can be covered by BS m, with the maximum range decided by a beam with the minimum beamwidth and maximum BS transmit power. Throughout the paper, we assume each BS is equipped with an antenna array with L antenna elements, and each UE has a single antenna. Note that BOON can be extended to accommodate UEs with multiple antennas.

Let K be the number of beamformers for each BS. Each beamformer can form one beam. Note that the required processing power, design complexity and fabrication cost of a BS grows with the number of beamformers; hence a BS can only have a limited number of beamformers. For each beam $k \in C_m$, let $\mathcal{U}_{mk} \subseteq \mathcal{U}_m$ be the set of UEs that are inside beam k of BS m, called as beam $\langle m, k \rangle$.

Many works on mmWave channel modeling consider both LOS and *non-line-of-sight* (NLOS) paths [2]–[4], [13], [24]. Nevertheless, multiple channel measurement experiments on mmWave frequency showed that the LOS path dominates the NLOS paths. For instance, the NLOS path gain is typically 20 dB weaker than the LOS path gain [20], [24]–[26] and the NLOS path exponent was found as large as

5.76 in downtown New York City [2]. In this paper, we focus on the LOS paths to streamline the algorithm development. We will extend our approach to address NLOS paths in our future work.

Let d_{mn} and ρ_{mn} denote the distance, and average LOS path loss, respectively, between BS m and UE n. Note that ρ_{mn} is often modeled as proportional to $d_{mn}^{-\eta}$, where η is the path loss exponent of the LOS path. Also let θ_{mn} be the normalized direction of the LOS path to reach UE n from BS m, as illustrated in Fig. 3, and α_{mn} be the complex gain of the LOS path which is modeled using a complex Gaussian distribution, i.e., $\alpha \sim \mathcal{CN}(0,1)$. Now the channel vector between the m-th BS with L antennas and the n-th UE ($n \in \mathcal{U}_{mk}$) with a single antenna is given as [19], [20], [24]

$$\mathbf{h}_{mn} = \sqrt{\frac{L}{\rho_{mn}}}\alpha_{mn}\mathbf{a}_{\theta_{mn}}, \tag{1}$$

where $\mathbf{a}_\theta$ is the response vector of the BS antenna array for the signal path in the θ direction. The response vector for a *uniform linear array* (ULA) at a BS is expressed as [19], [20], [24]

$$\mathbf{a}_\theta = \frac{1}{\sqrt{L}}\left[1, \quad e^{-j\pi\theta}, \ldots e^{-j\pi(L-1)\theta}\right]^T, \tag{2}$$

where $(\bullet)^T$ denotes transpose of a vector. Note that the normalized direction θ is a function of the physical *angle of departure* of the BS antenna array, denoted by $\phi \in [-\pi/2, \pi/2]$, as $\theta = \frac{2\Delta\sin(\phi)}{\lambda}$, where λ is the channel frequency wavelength and Δ is the spacing between two adjacent antenna elements in a ULA. Concatenated channel matrix formed by all UEs in BS m is therefore written as

$$\mathbf{H}_m = [\mathbf{h}_{m1}, \mathbf{h}_{m2}, \ldots, \mathbf{h}_{mn}], \quad n \in \mathcal{U}_m \tag{3}$$

The received signals in all UEs under BS m is given by

$$\mathbf{Y}_m = \mathbf{H}_m^H \mathbf{W}_m \mathbf{x}_m + \mathbf{z}, \tag{4}$$

where $(\bullet)^H$ denotes the complex conjugate transpose, $\mathbf{x}_m \in \mathbb{C}^{|\mathcal{U}_m|\times 1}$ is the vector of transmitted signals for UEs in BS m, $\mathbf{z} \in \mathbb{C}^{|\mathcal{U}_m|\times 1}$ is the vector of Additive White Gaussian Noise (AWGN) with zero mean and unit variance, $\mathbf{W}_m \in \mathbb{C}^{L\times|C_m|}$ is the beamforming weight matrix formed by concatenating weight vectors, $\mathbf{w} \in \mathbb{C}^{L\times 1}$, in BS m, i.e., $\mathbf{W}_m = \left[\mathbf{w}_{m1}, \mathbf{w}_{m2}, \ldots, \mathbf{w}_{m|C_m|}\right]$.

3.2 Downlink Transmit Power

In BOON, each BS constructs a set of unit-power beams, denoted by $\{\mathbf{w}_{m1}, \ldots, \mathbf{w}_{m|C_m|}\}$, i.e., the power in each beam $||\mathbf{w}||^2 = 1$. As illustrated in Fig. 3, each beam serves a group of UEs. Let $\hat{\theta}_{mk}$ denotes the main lobe direction (boresight angle) of the beam $\langle m,k\rangle$ formed by $\mathbf{w}_{mk}$ to serve all UEs in $\mathcal{U}_{mk}$. The effective channel gain of UE $n \in \mathcal{U}_{mk}$ from beam $\langle m,k\rangle$ can be written as [19], [20]

$$|\mathbf{h}_{mn}^H \mathbf{w}_{mk}|^2 \approx \frac{|\alpha_{mn}|^2}{\rho_{mn}} F_L(\hat{\theta}_{mk} - \theta_{mn}), \tag{5}$$

where $(\bullet)^H$ denotes the complex conjugate transpose, α_{mn} is the complex gain of the LOS path between BS m and UE n, ρ_{mn} is the average LOS path loss between BS m and UE n, and $F_L(x)$ is the Fejér kernel [19]. If $(\hat{\theta}_{mk} - \theta_{mn}) \to 0$, the UE channel gain is at maximum.

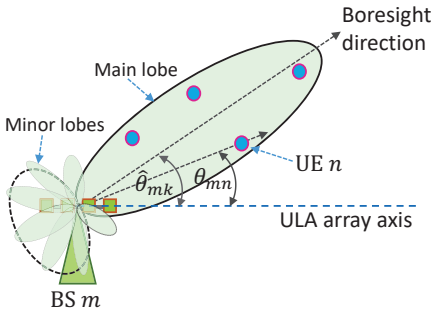

Fig. 3. One beam to cover a group of nearby UEs. $\hat{\theta}_{mk}$ and θ_{mn} denote the boresight direction of beam $\langle m,k\rangle$ and the direction of UE n, respectively.

Let p_{mk}^t be the transmit power of beam $\langle m,k\rangle$. The received signal power at UE n from beam $\langle m,k\rangle$, denoted as $p_{n,m,k}^r$, is written as

$$p_{n,m,k}^r = p_{mk}^t |\mathbf{h}_{mn}^H \mathbf{w}_{mk}|^2, \quad \forall n \in \mathcal{U}_{mk}. \tag{6}$$

Let $I_{n,m,k}$ denote the total interference at UE n from all beams, if it is covered by beam $\langle m,k\rangle$. Let σ^2 be the thermal noise at a UE, which is modeled as $\sigma^2 = N_o + 10log(w) + \text{NF}$, where w is the system bandwidth, N_o is the noise power spectral density and NF denotes the noise figure at the UE receiver. The SINR at UE n from beam $\langle m,k\rangle$ is written as

$$\gamma_{n,m,k} = \frac{p_{n,m,k}^r}{I_{n,m,k} + \sigma^2}. \tag{7}$$

To achieve a certain quality of service for the UE, the SINR at the UE has to be greater than or equal to a minimum SINR γ_o. Thus, we need to have

$$\frac{\gamma_{n,m,k}}{\gamma_o} \geq 1, \quad \forall n \in \mathcal{U}_{mk}. \tag{8}$$

In order to maintain the minimum γ_0 at all UEs in a beam, the required transmit power p_{mk}^t is obtained using (6)-(8) as

$$p_{mk}^t \geq \frac{(I_{n,m,k} + \sigma^2)\gamma_o}{|\mathbf{h}_{mn}^H \mathbf{w}_{mk}|^2}, \quad \forall n \in \mathcal{U}_{mk}. \tag{9}$$

The transmit power vector for all beams of BS m is given by

$$\mathbf{p}_m^t = \left[p_{m1}^t, p_{m2}^t, \ldots, p_{m|C_m|}^t\right], \tag{10}$$

where $|x|$ denote the cardinality of set x. Our objective is to reduce the total transmit power

$$\sum_{m\in B, i\in C_m} p_{mi}^t. \tag{11}$$

3.3 Downlink UE Rate

The beam radiation patterns in the real world are complicated. Fig. 4 depicts a network with 2 BSs and 4 beams, with beam A transmitting to UE2, and beam B transmitting to UE1 and UE3. While UE1 is covered by beam B, it may receive *intra-BS interference* from beam A, e.g., if the null of beam A is not perfectly aligned with UE1. UE3 has *inter-BS interference* from beam D.

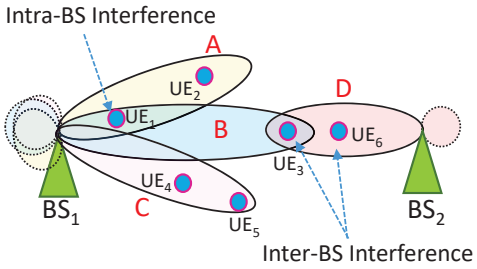

Fig. 4. Inter-BS interference at UE3 and intra-BS interference at UE1

We quantify both intra-BS interference and inter-BS interference for a UE. For UE n served by beam $\langle m,k\rangle$, the total interference $I_{n,m,k}$ is the summation of intra-BS interference $I'_{n,m,k}$ and inter-BS interference $I''_{n,m,k}$ given as follows.

$$I_{n,m,k} = I'_{n,m,k} + I''_{n,m,k} = \sum_{i\in C_m\setminus k} p^r_{n,m,i} + \sum_{j\in B\setminus m}\sum_{l\in C_j} p^r_{n,j,l}$$
$$= \sum_{i\in C_m\setminus k} p^t_{mi}|\mathbf{h}^H_{mn}\mathbf{w}_{mi}|^2 + \sum_{j\in B\setminus m}\sum_{l\in C_j} p^t_{jl}|\mathbf{h}^H_{jn}\mathbf{w}_{jl}|^2 \quad (12)$$

In (12), the first term $I'_{n,m,k}$ is the summation of powers received by UE n from all beams in C_m except the serving beam k. The second term $I''_{n,m,k}$ is the sum of powers received from the beams of other BSs, i.e., except the serving BS m. Note that we compute the received power for a UE using (6).

The throughput capacity of the downlink channel has to be shared among all UEs in a beam. UEs in the same beam can use any multiplexing scheme to share resources, e.g., TDMA (time division multiple access), OFDMA (orthogonal frequency division multiple access), or NOMA (non-orthogonal multiple access). In the ensuing discussions, we assume the OFDMA system, but it can be similarly done for NOMA and TDMA. In this paper, we assume a fair resource allocation similar to LTE, i.e., the OFDM sub-carriers are shared equally among UEs in a beam. If UE n is scheduled in beam $\langle m,k\rangle$, the rate of UE n in each downlink frame is given as

$$r_{n,m,k} = w_n \log_2(1+\gamma_{n,m,k}), \quad (13)$$

where w_n is the sum of frequency spectrum from all downlink sub-carriers assigned to UE n in the beam, and $\gamma_{n,m,k}$ is the corresponding SINR given by (7). If w is the total system bandwidth, $w_n = w/|\mathcal{U}_{mk}|$, where $|\mathcal{U}_{mk}|$ denotes the number of UEs in the beam $\langle m,k\rangle$. The sum rate of the network is given as

$$\sum_{m\in B, 1\le k\le K, n\in\langle m,k\rangle} r_{n,m,k} \quad (14)$$

4 Beamforming Oriented Topology Control (BOON)

Our objective for topology control is to reduce the total transmit power in (11), subject to coverage of all UEs, maintaining the minimum SINR at each UE by (9), and using no more than the maximum number of beamformers at each BS. Moreover, for a given transmit power that meets those constraints, we aim to increase the sum rate in (14). We take a heuristic approach to achieve these two objectives. To reduce the transmit power, we first group UEs together through a *beamforming oriented UE clustering* (BOC) algorithm. This clustering is with regard to each BS assuming the maximum range and the clusters are formed with a radial shape with the center at a BS. The clusters of different BSs may overlap with each other, i.e., some UEs are included in clusters of different BSs. To associate those overlapped UEs to the right BSs, we divide each cluster into finer granularity sets through a *cluster decomposition based set construction* (CDSC) algorithm. Next, we associate these sets to the BSs through an *interference aware set covering* (IASC) algorithm, which selects a list of sets that cover all UEs, but do not overlap. Such UE/set association thus avoids or reduces interference between BSs, which reduces the transmit power of the BSs and increases the sum rate. At last, one beam is formed to cover each set by its associated BS. In the following, we describe each of those steps, which form the four components of BOON.

4.1 Beamforming Oriented UE Clustering (BOC)

From the topology control perspective, clustering is a process of organizing UEs into groups based on a similarity or cost metric. Clustering is in general NP-hard [27]. In this section, we develop a heuristic algorithm to find the number of clusters and their UEs for a BS, with the objective to reduce the transmit power of the BS. UEs are grouped based on their angles relative to the BS and the UE-UE distance.

Algorithm 1 illustrates the BOC algorithm that iteratively clusters UEs for a BS. BOC is a heuristic greedy algorithm which iteratively reduces the total clustering cost in each successive stage. It starts with each UE as one cluster. Two or more clusters are merged into one cluster in each successive stage, until the number of clusters is up to the number of beamformers K of a BS or the cost does not decrease any more. The output is the optimal number of clusters and UE set $\mathcal{U}_{mk}$ in each cluster. In order to assess if we should merge two clusters i and j into a new cluster (i,j) in an iteration, we compute the cost metric for the new cluster. The cost metric determines the performance of BOC. In this paper, we use a cost metric based on *energy efficiency* (EE) in bit/joule. EE measures the amount of downlink rate that a beam can deliver with per unit energy in joule it consumes. The clustering cost metric is the inverse of EE since our goal is to reduce transmit power in the network. Specifically, the cost of cluster (i,j) is defined as

$$c_{(i,j)} = \frac{p^t_{(i,j)}}{\sum_{n\in\mathcal{U}_{(i,j)}} w_n \log_2\left(1+\frac{p^t_{(i,j)}|\mathbf{h}^H_n\mathbf{w}_{(i,j)}|^2}{I_{n,(i,j)}+\sigma^2}\right)}, \quad (15)$$

where $p^t_{(i,j)}$ is the transmit power, $I_{n,(i,j)}$ is the received interference at UE n given by (12), and $\mathbf{w}_{(i,j)}$ is the weight vector.

While it is straightforward to consider all possible pairs of clusters for merging, in practice the beamforming gain is negligible when the main lobe is very wide. For instance, the approximate beamforming gain is $\pi^2/(\phi^{hp})^2$, where ϕ^{hp} is the solid angle for both the azimuth and elevation plane

Algorithm 1: Beamforming oriented clustering (BOC) for a BS

1 **Input:** UE set $\mathcal{U}$ and maximum number of beams K
2 Let each UE be a cluster, with the set of clusters $\mathcal{B} = \{\{1\}, \{2\}, \dots \{|\mathcal{U}|\}\}$
3 Let $v = K$, and Let cost vectors $\mathbf{c} = \mathbf{0}$ and $\bar{\mathbf{c}} = \mathbf{0}$
4 **while** $|\mathcal{B}| \geq v$ *or* $\sum \mathbf{c} < \sum \bar{\mathbf{c}}$ **do**
5 $\bar{\mathcal{B}} \leftarrow \mathcal{B}$, $\bar{\mathbf{c}} \leftarrow \mathbf{c}$
6 **if** $|\mathcal{B}| = 1$ **then**
7 break out of loop
8 **end**
9 For each cluster s and the next clusters k within angle φ in the angular space, compute $c_{(s,k)}$ using (15)
10 Select two clusters $(i, j) = \underset{s,k}{\operatorname{argmin}}\ c_{(s,k)}$
11 Update $\mathcal{B}$: create a new cluster h for $\mathcal{B}$ to replace clusters i, j in $\mathcal{B}$. If the beam to cover UEs in cluster h also covers a UE in a different cluster (not i or j), then merge that cluster into cluster h
12 Update $\mathbf{c}$ to be the cost vector of clusters in $\mathcal{B}$
13 **end**
14 Output $\bar{\mathcal{B}}$ as the set of clusters

[28]. We choose a feasible value of φ such that beyond which the UE channel gain is very small and beamforming becomes inefficient. Hence, in line 8 of Algorithm 1, we actually do not need to consider all possible pairs. Instead, for a cluster, we only consider the next few clusters within angle φ in the angular space for possible merging. At last, we choose one pair to merge into one cluster which yields the lowest cost.

A challenge for BOC is that the UE set in the merged cluster (i, j) is not necessarily the combined UEs from clusters i and j together. This is different from classic clustering. Let $\mathcal{U}_{(i,j)}$ denote the UE set of the new cluster (i, j). For classic clustering, if an object $x \notin \mathcal{U}_i$ and $x \notin \mathcal{U}_j$, then we must have $x \notin \mathcal{U}_{(i,j)}$. However, in BOC, there may exist a UE x such that $x \notin \mathcal{U}_i$ and $x \notin \mathcal{U}_j$, but $x \in \mathcal{U}_{(i,j)}$. As an example, we consider three clusters (or beams) A, B, and C, in the network illustrated in Fig. 4. Suppose clusters A and C are selected to be merged. Then to avoid beams overlapping, we have to let the new cluster (A,C) to serve UE3, even though it is not in cluster A or C. Therefore, in line 10, we check if a cluster in between needs to be merged with clusters (i, j).

A benefit of the above cost metric is that it can help to automatically find the optimal number of clusters, which corresponds to the lowest clustering cost. There is a trade-off between the number of UEs in a cluster and the total number of clusters for a BS. More UEs in a cluster reduce the spectral share per UE, which results in a higher clustering cost. On the other hand, more clusters mean fewer UEs in a cluster, which increases the UE spectral share. Nevertheless, this in turn increases the interference between beams, also resulting in a higher clustering cost. By 'minimizing' the clustering cost, BOC automatically selects the optimal number of clusters. This is done through continuously merging clusters even after the number of clusters reaches K, the number of beamformers at a BS. The algorithm terminates when the total cost $\sum \mathbf{c}$ does not decrease anymore, i.e., the clustering cost of the current iteration $\sum \mathbf{c}$ is higher than the one of the previous iteration $\sum \bar{\mathbf{c}}$ in line 4.

If N UEs are distributed separately from each other in the angular space with regards to the BS, such that the difference between two neighbor UEs is greater than φ, each UE forms one cluster, where K is the number of beamformers for the BS, and φ is the threshold for the main lobe width of a beam. BOC only needs to compute the clustering cost for each of the N UEs once. Thus, the time complexity is $\Theta(N)$. However, in the worst case, BOC may need to run $N - 1$ iterations for merging clusters. In each iteration, BOC needs to compute $\Theta(N_j)$ cost metrics, where N_j is the number of clusters in the jth iteration, since for each cluster s, we only need to consider the next few clusters, as discussed above. Thus, the worst-case time complexity of BOC is $\mathcal{O}(N^2)$.

4.2 Cluster Decomposition based Set Construction (CDSC)

The BOC algorithm groups UEs into clusters for each BS independently. In a multi-BS network, we cannot form beams directly based on those clusters, because clusters from different BSs can overlap with each other, which causes significant inter-BS interference. Therefore, we develop a *cluster decomposition based set construction* (CDSC) scheme to decompose each cluster into a number of sets. The objective is to avoid inter-BS interference for formed beams. For instance, in Fig. 5(a), UE a can be covered by both BS1 and BS2, and thus is clustered by both BS1 and BS2. If we form beams directly based on clusters, the two beams interfere each other. Through constructing sets as in Fig. 5(c) or (d), we can let BS1 form a beam to cover set B, which then eliminates interference between BS1 and BS2.

Different set construction schemes produce different beams which result in different transmit power. A naive approach is the *exhaustive set construction* (ESC). With ESC, we start from the closest UE of a cluster in the radial direction and contiguously construct one set per UE outward, with each set being a true superset of the previous set. For instance, suppose there are three UEs $(1, 2, 3)$ in a cluster for a BS, with UE 1 the closest, and UE 3 the farthest to the BS. The ESC scheme constructs three sets from this cluster, $C = \{1\}$, $B = \{1, 2\}$, and $A = \{1, 2, 3\}$. While ESC is easy to be implemented, it may generate a large number of sets, which results in a large running time for set covering in the next step of BOON. Hence, we develop another scheme, termed *shrinkable set construction* (SSC), to reduce the number of sets generated by set construction.

Fig. 5 illustrates ESC and SSC with six UEs (a, b, c, d, e, f) forming four clusters with four BSs. For each cluster of a BS, we first identify the *intersections* between this cluster and the clusters of other BSs, by looking at the common UEs between them. Then the cluster is partitioned into intersection areas and non-intersection areas, as illustrated in Fig. 5(b). The intuition behind partitioning UEs into intersection and non-intersection areas is that UEs in the intersection areas can be associated with either BS, but UEs in the non-intersection area can be associated with only one BS. For example, in Fig. 5, UE a forms an intersection area

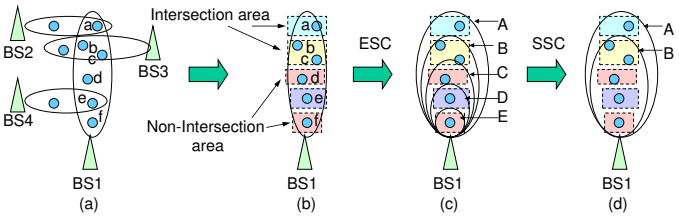

Fig. 5. Exhaustive set construction (ESC) and shrinkable set construction (SSC)

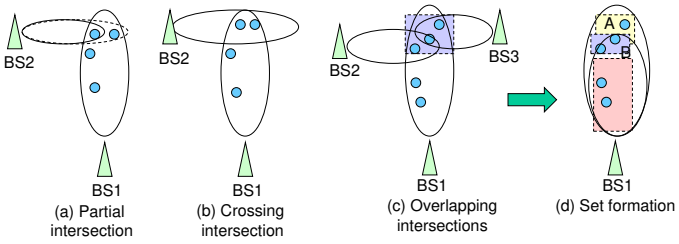

Fig. 6. Intersection areas

and can be associated with either BS1 or BS2. UE d forms a non-intersection area, and can be associated with BS1 only. We group the UEs in an intersection area into an *atomic set*. The UEs in a non-intersection area are also grouped into an atomic set. For example, there are five atomic sets in Fig. 5(b). Three atomic sets $\{a\}, \{b, c\}, \{e\}$ are formed by intersection areas and two atomic sets $\{d\}, \{f\}$ are formed by non-intersection areas. We then treat each atomic set as a UE, and apply the ESC scheme to construct sets, as illustrated in Fig. 5(c). Note that each set is constructed by concatenating a sequence of contiguous atomic sets starting from the one closest to the BS and going outward.

The intersection between clusters can be more complicated than the case in Fig. 5. We illustrate three complicated intersection cases: *partial intersection*, *crossing intersection*, and *overlapping intersection* in Fig. 6. With partial intersection, we can extend the intersection area to become a full intersection, illustrated by the extended dotted line in Fig. 6(a). This is done by letting the BS slightly increase the transmit power to cover the UEs in the dotted line. The scenario with crossing intersection is treated as the same as full intersection. For the overlapping intersection with two or more other BSs, as illustrated in Fig. 6(c), we start from the intersection area closest to the BS, and let all UEs in this area be an atomic set. We remove the overlapped part of this intersection area with the next intersection area, and let the remaining UEs in the next intersection area be the next atomic set, as illustrated in Fig. 6(d).

The main idea of the SSC scheme is to remove some sets formed by ESC to reduce the total number of sets, as illustrated in Fig. 5(d). This may significantly reduce the running time of the set covering algorithm in the next section. First of all, we define the concept 'shrinkable'. A set Y is *shrinkable* to its direct subset X, iff the atomic set $s = Y \setminus X$ is an intersection area. The core idea of SSC is that if Y is *shrinkable* to X, then X can be removed, without affecting the set covering result. We explain the intuition through an example illustrated in Fig. 5. As discussed earlier, an atomic set in a non-intersection area is covered by only one BS, but an atomic set in an intersection area can be covered by more than one BS. If the set covering algorithm (to be discussed in the next section) first selects the outermost atomic set $\{a\}$ of set A to be covered by BS2, then for BS1, set A will automatically shrink to set B. Hence, in the very beginning, we do not need to have set B in the initial sets for the set covering algorithm. That is, the set covering result does not change even if we remove set B in the initial sets. On the other hand, if the set covering algorithm selects atomic set $\{e\}$ in set C to be covered by BS4, then set C cannot shrink to set D or E because the atomic set $\{d\}$ in C has to be covered by BS1. In summary, a set Y is *shrinkable* to its direct subset X, iff the atomic set $s = Y \setminus X$ is an intersection area. The following theorem states whether a set can be removed before feeding the sets to the set covering algorithm.

Theorem 1. *Consider a set Y and its direct subset X constructed from the same cluster, i.e., $Y \setminus X$ contains only one atomic set. We can remove X without affecting the set covering results, if any of the following conditions are satisfied.*

1) *X is not shrinkable.*
2) *X is shrinkable, but Y is not shrinkable.*

Proof. First of all, with condition 1, we must have that set Y is shrinkable. It is not possible that both X and Y are not shrinkable, based on the construction of beamforming sets. This is because if this is the case, then the outmost two atomic sets in set Y are both in non-intersection areas, which is in conflict with the partitioning of a cluster into intersection and non-intersection areas. We use an example to illustrates X and Y. Consider sets B and C in Fig. 5(c), which correspond to Y and X. Furthermore, let set Z denote the set from another cluster that intersects with the outmost atomic set of set Y. With set Y as shrinkable, if the set covering algorithm selects set Z first (before selecting Y), set Y can shrink to set X. That is, even if set X was removed, shrinking Y essentially re-creates set X, which could be selected by the set covering algorithm later. Thus the set covering is not affected even if set X was removed. On the other hand, if the set covering algorithm selects set Y first, we do not have to keep set X since set X would not be selected anyway by the set covering algorithm, because selecting set Y implies the UEs in set X are already covered. Hence condition 1 is a sufficient condition to remove set X.

With condition 2, the outmost atomic set s in Y, where $s = Y \setminus X$, is in a non-intersection area. Hence the UEs in the atomic set s cannot be served by another BS. So the BS that set Y belongs to has to cover atomic set s, which implies that set Y is covered. This in turn implies set X would not be selected by the set covering algorithm later on. It is possible that if we do not remove set X, the set covering algorithm may select set X before selecting set Y. However, eventually the set covering algorithm has to select set Y or its superset, to cover the atomic set s. Thus, set X would be removed since its superset is selected. That is, we can remove set X in the beginning, without affecting the set covering result. ■

4.3 Interference Aware Set Covering (IASC)

While set covering is a classic problem, the inter-beam interference raises a great challenge to applying set covering

Algorithm 2: Interference aware set covering (IASC)

1 **Input:** Set family $\mathcal{F}$, set costs $c(\mathcal{S})$, UE set $\mathcal{U}$
2 $\mathcal{C} = \emptyset$
3 **while** $\mathcal{U} \neq \emptyset$ **do**
4 $\mathcal{S} = \text{argmin}_{x \in \mathcal{F}}\, c(x)$
5 Remove UEs of $\mathcal{S}$ from $\mathcal{U}$
6 $\mathcal{F} \leftarrow \mathcal{F} \setminus \mathcal{S}$
7 **for** *each set* $x \in \mathcal{F}$ **do**
8 **if** *x shrinks when we remove $\mathcal{S}$* **then**
9 Remove all UE $i \in x \cap \mathcal{S}$ from x and update $c(x)$
10 **end**
11 **end**
12 Remove any set h in $\mathcal{C}$ if $h \subset \mathcal{S}$
13 Add set $\mathcal{S}$ to $\mathcal{C}$
14 **end**
15 **return** $\mathcal{C}$

for beamforming. A major difference is that, in classic set covering, the objects in the selected set in a given step are removed from the remaining sets, which is a key technique to optimize performance in classic set covering. Unfortunately, IASC cannot use this technique, as removing UEs from the remaining sets may cause strong interference in the later beamforming stage. In fact, with IASC, there is only one scenario where we can remove a UE from the remaining sets. That is, if a remaining set is *shrinkable*, we can remove a UE from it. This is because, when the set *shrinks*, the cost of the remaining set is recalculated and updated. If it results in a strong interference, the cost will be high. Hence this shrunk set would be unlikely selected in the future steps of set covering.

Algorithm 2 illustrates the IASC algorithm. Let $\mathcal{S}_i$ denote the ith SSC set after applying the CDSC scheme in BOON. Note that $\bigcup_i \mathcal{S}_i = \mathcal{U}$. All SSC sets of all BSs are denoted as $\mathcal{F} = \{\mathcal{S}_i\}$. We use (15) to compute the cost for set $\mathcal{S}_i$, denoted as $c(\mathcal{S}_i)$. The objective of IASC is to find an index subset $J \subseteq \{1, 2, \ldots, |\mathcal{F}|\}$ such that $\sum_{i \in J} c(\mathcal{S}_i)$ is minimum, subject to $\bigcup_{j \in J} \mathcal{S}_j = \mathcal{U}$. Initially, the algorithm lets $\mathcal{C}$ be empty. IASC picks a set $\mathcal{S}$ with the minimum cost in each iteration, and remove UEs of this set from $\mathcal{U}$ (note that not from other remaining sets in $\mathcal{F}$). The selected set $\mathcal{S}$ is then removed from $\mathcal{F}$. Next, we check if any $x \in \mathcal{F}$ is "shrinkable" if we remove UEs of $\mathcal{S}$ from x. If x can "shrink", we remove the common UEs in both $\mathcal{S}$ and x, i.e., $x = x \backslash \mathcal{S}$, and update the cost $c(x)$. If x cannot shrink, we do not remove any UE from x even though a UE is already covered by $\mathcal{S}$, based on earlier discussions. Next we check if set $\mathcal{S}$ covers all UEs in a previously selected set h. If yes, we remove set h from $\mathcal{C}$. Finally $\mathcal{S}$ is added to $\mathcal{C}$. The algorithm outputs a list of sets with the minimal total cost, while all UEs are covered by those sets. In summary, IASC tries to reduce the overall network cost while minimizing the set overlapping such that each UE is associated with one beam.

Set covering is an NP-hard problem. The IASC algorithm is a heuristic greedy algorithm to solve the weighted set covering problem. In each iteration, the time is mainly on updating the set cost on line 7, which requires $\mathcal{O}(|\mathcal{F}|)$ time. The worst case run time of IASC is $\mathcal{O}(|\mathcal{U}||\mathcal{F}|)$.

4.4 Beamforming

We adopt the *linearly constrained minimum variance* (LCMV) beamforming scheme [29, p.513]. It is able to constrain the beamforming output to achieve a given gain in the directions of intended UE signals while minimize the power response toward UE directions in other beams and BSs. To achieve a complex gain g^* in the UE direction θ, the beamforming weight vector is subject to $\mathbf{a}_\theta^H \mathbf{w} = g^*$, where $\mathbf{a}(\bullet)$ is given by (2). Let $\mathbf{A}_\theta = [\mathbf{a}_{\theta_1}, \ldots, \mathbf{a}_{\theta_k}]$ be the constraint matrix for total k UEs of a BS, with AoAs $\theta_1, \ldots, \theta_k$, and $\mathbf{f}$ be the k-dimension single column response vector. The covariance of the k UE signals $\mathbf{R} = \mathbb{E}\left[\mathbf{h}\mathbf{h}^H\right] = \frac{L|\alpha|^2}{\rho}\mathbf{A}_\theta \mathbf{A}_\theta^H$, where $\mathbf{h}$ is the k UE channel vectors given in (1), L is number of antenna elements in the BS, ρ is the path loss and α is the complex gain of the signal. The LCMV beamforming to minimize transmit power is formulated as

$$\min\{\mathbf{w}^H \mathbf{R} \mathbf{w}\} \text{ such that } \mathbf{A}_\theta^H \mathbf{w} = \mathbf{f}. \tag{16}$$

The solution of (16) is obtained as follows using the Lagrange multiplier method

$$\mathbf{w} = \mathbf{R}^{-1}\mathbf{A}_\theta(\mathbf{A}_\theta^H \mathbf{R}^{-1} \mathbf{A}_\theta)^{-1}\mathbf{f}. \tag{17}$$

By clustering UEs into groups and choosing an appropriate beamforming weight vector for each group, it is possible to approximately eliminate or significantly reduce the inter-beam interference. The time complexity of the LCMV beamforming in (17) is $\Theta(\max(kL^2, L^{2.373}))$ assuming $L \geq k$, where $L^{2.373}$ is the matrix inverse time for an $L \times L$ matrix.

We use the channel vector $\mathbf{h}_{mn}$ between BS m and UE n in (1) to compute a beamforming weight vector $\mathbf{w}$ for each set in $\mathcal{C}$ output by IASC, to serve all UEs in this set. Let $\mathcal{U}_i$ denote the UEs contained in the ith set in $\mathcal{C}$. Also let m_i denote the corresponding BS of set $\mathcal{C}_i$, i.e., the ith set in $\mathcal{C}$. For each UE set $\mathcal{U}_i$, we construct the constraint matrix $\mathbf{A}_\theta$, the corresponding covariance matrix $\mathbf{R}$, and the response vector $\mathbf{f}$. Then we use (17) to compute $|\mathcal{C}|$ number of weight vectors $\mathbf{w}_1, \ldots, \mathbf{w}_{|\mathcal{C}|}$, where $\mathbf{w}_i$ is associated with set $\mathcal{C}_i$. Then using (9), the transmit power allocated to the signal for set $\mathcal{C}_i$ is computed as

$$p_i^t = \max\left(\frac{(I_n + \sigma^2)\gamma_o}{|\mathbf{h}_{m_i,n}^H \mathbf{w}_i|^2}\right), \quad \forall n \in \mathcal{U}_i, i \in \mathcal{C} \tag{18}$$

where $\mathbf{h}_{m_i,n}$ is the channel vector between BS m_i and UE n, γ_o is the required minimum SINR threshold for all UEs, and σ_n^2 is the noise power in the AWGN channel for UE n. Note that interference I_n in (18) is close to zero because IASC finds the best sets of UEs to avoid interference. Furthermore, the beamformer constraint and response vector are applied to form null in the direction of UEs of other sets.

5 Performance Evaluation

We compare BOON with MUB, MCB based topology control, and a state-of-the-art scheme JSDM [13]. All schemes use the same beamforming technique, LCMV. Note that both MUB [8], [9], [20], [30] and MCB [10]–[12], [31] are special cases of BOON. The former treats each UE as a set, forming one dedicated beam for each UE, while the latter treats all UEs in one set, i.e., forming one beam to serve all UEs. In JSDM, UEs are partitioned into groups with

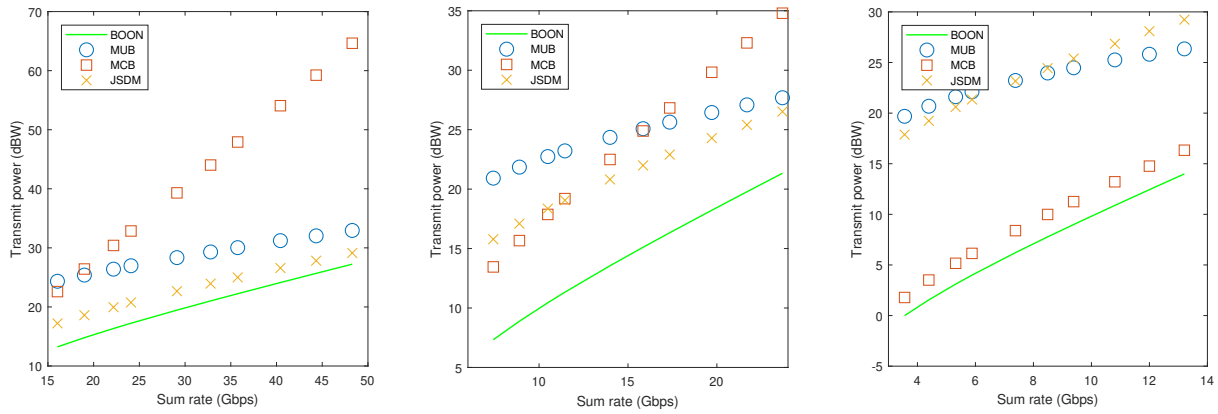

Fig. 7. Average sum rate versus transmit power of 50 experiments: (a) spread UE distribution (b) grouped UE distribution, (c) dense UE distribution. $\gamma_0 = 1$ to 15 dB.

TABLE 2
Simulation parameters

Parameter	Value
System operating frequency (GHz)	73
Network dimension (m^2)	$[400 \times 200]$
Number of antennas in ULA per BS	16
Adjacent antenna spacing Δ in ULA	$\lambda/2$
Maximum number of beamformers K per BS	10
System bandwidth (FDD duplex mode) (MHz)	500
LOS path loss exponent η	2.2
Minimum required SINR γ_o at UE (dB)	1 to 15
Noise power spectral density N_o (dBm/Hz)	-174
Noise figure NF at UE receiver (dB)	6

TABLE 3
Average required transmit power of BOON (in %) with respect to MUB, MCB, and JSDM, to achieve the same average sum rate

UE Pattern	Gbps	vs. MUB	vs. MCB	vs. JSDM
Spread	31.2	15.08 %	2.71 %	50.37 %
Grouped	15.05	10.87 %	12.9 %	20.6 %
Dense	8.03	3.3 %	80.4 %	2.9 %

approximately similar channel covariances. All UEs in a group are served simultaneously using one beamforming vector. We assume all BSs are configured with a ULA, while each UE is equipped with a single antenna. The OFDMA system is assumed for spectrum sharing among UEs in a beam. We consider a frequency division duplex (FDD) mode where 80% of the system bandwidth, i.e., 400 MHz, is used for downlink data signal transmission and the rest 20% is used for control signal purpose. The system parameters used in simulations are summarized in Table 2. The performance metrics we use are the BS transmit power, sum rate of all UEs, SINR, and computation complexity. The sample networks are in a $[400 \times 200]$ m^2 outdoor area, with 6 BSs and 40 UEs. There are 10 blockages in four different shapes, rectangle, square, hexagon, and pentagon. The *reference signal received power* based UE association is used in MUB, MCB, and JSDM. The BSs are evenly distributed in the network area. UEs are distributed by three patterns; *spread*, *grouped*, and *dense*. In the spread UE distribution, UE locations are randomly distributed. In the grouped UE distribution, 40 UEs form into 10 UE groups, each with 4 UEs. The center of each group is randomly generated, and the 4 UE locations are randomly generated, but closely located to the center. In the dense UE distribution, UEs form into one to two groups around each BS. The group center and UE locations are generated similarly as in the grouped UE distribution.

We have generated 50 networks for each UE distribution pattern, respectively. We record the average transmit power and sum rate for each network. The required minimum SINR γ_o varies in a range of 1 to 15 dB. In simulations, we first find the transmit power for BOON to meet a minimum SINR γ_o at every UE and record the corresponding sum rate. Then we apply the same transmit power in MUB, MCB and JSDM to find their SINR and sum rate. Fig. 7 illustrates the *scatter plot* of the average sum rate versus transmit power for 50 networks/experiments in each UE distribution pattern, using different seeds for simulations. Each data point in the figure indicates the required transmit power for each scheme to achieve a given sum rate. The average error bar length (95% confidence interval) of BOON, MUB, MCB, and JSDM is 2.3, 3.2, 3.5, and 4.8 dBW, respectively. They are not plotted in the figure as the error bars of different schemes overlap with each other significantly, which makes them hard to be viewed. Overall, BOON significantly outperforms other schemes, thanks to the effective BOC clustering, and the IASC algorithm which smartly associates UEs to BSs to avoid inter-BS interference. BOON not only uses less transmit power, but also has a smaller error bar. In the dense UE distribution, BOON performs similarly as MCB as it is best to form one or two beams in this case. They perform significantly better than MUB and JSDM, as the latter form multiple beams even for one group, and results in significant interference between UEs. *In summary, BOON smartly adapts to different UE distributions to achieve the best performance in all scenarios. Other schemes cannot adapt to different UE distributions, and thus perform well in certain scenarios, but perform poorly in other scenarios.*

In Table 3, we average the percentage transmit power BOON uses in all experiments, compared with MUB, MCB,

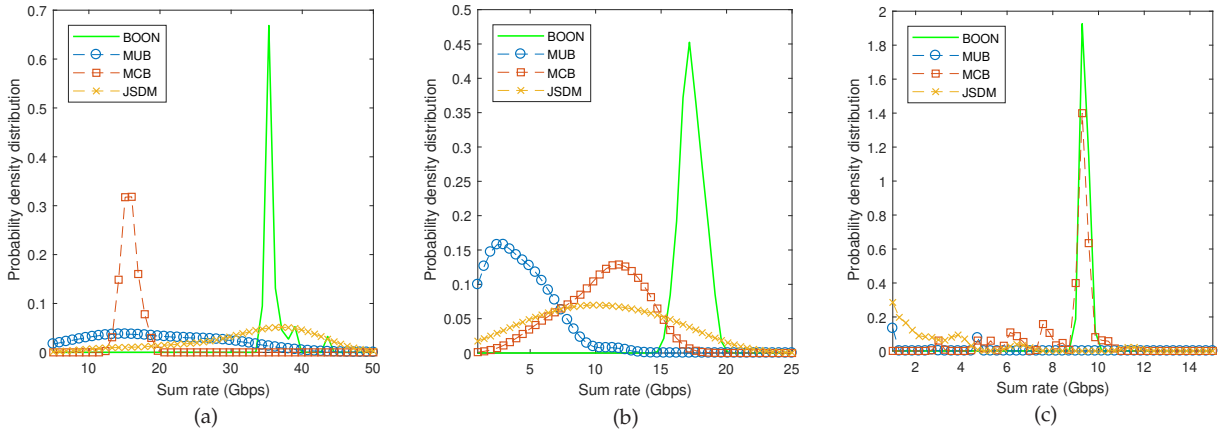

Fig. 8. Probability density distribution of the sum rate, (a) spread UE distribution, (b) grouped UE distribution, and (c) dense UE distribution, $\gamma_0 = 10$ dB.

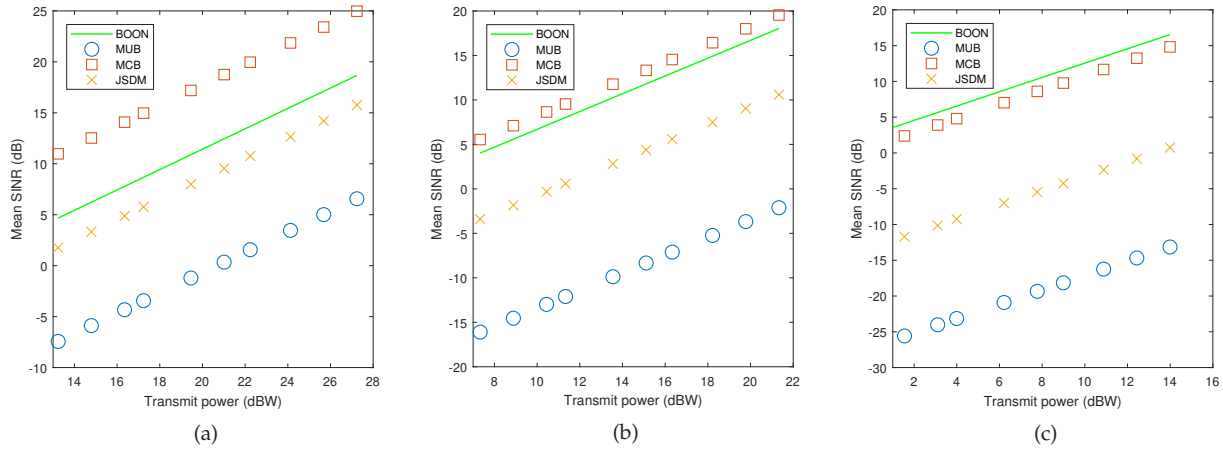

Fig. 9. The mean SINR versus transmit power of 50 experiments, (a) spread UE distribution, (b) grouped UE distribution, and (c) dense UE distribution. $\gamma_0 = 1$ to 15 dB.

and JSDM, to achieve the same sum rate. On average, BOON requires 10%, 32%, and 25% transmit power of MUB, MCB, and JSDM, respectively, to achieve an average 0.45 Gbps per UE rate. In other words, BOON achieves 90%, 68% and 75% gain in transmit power compared with MUB, MCB, and JSDM, respectively.

Fig. 7 only gives the average result among 50 experiments. Next we examine how spread the performance is across experiments. Fig. 8 plots the *probability density distribution* (PDF) of the sum rate obtained from the results of the 50 experiments for each UE distribution pattern, when the required minimum SINR $\gamma_o = 10$ dB. The PDF of the sum rates with different values of γ_o have similar trends and are omitted due to the space limitation. From Fig. 8, BOON not only achieves a higher average sum rate than MUB, MCB and JSDM, which can be verified by Fig. 7, but also has a much narrower spread on the sum rate overall. This indicates that for the 50 experiments, BOON can achieve most sum rates close to the average sum rate. In contrast, for JSDM and MUB, not only the average sum rate is smaller, but also the sum rates are much more spread out. This means that for some networks, their sum rates are very poor, significantly smaller than the average, while for some other networks, their sum rates are much higher than the average. In other words, their performance highly relies on the specific UE location distribution. *This is another demonstration that BOON smartly adapts to all network scenarios or UE location distributions, to achieve a good performance in all scenarios, while other schemes cannot adapt to different network scenarios well.* Note that although MCB also has a relatively narrow spread, its sum rate is much lower than BOON, except in the dense UE distribution pattern.

Fig. 9 plots the average value of the mean SINR of the 50 experiments in each UE distribution pattern. BOON clearly outperforms JSDM and MUB. The average error bar length of BOON, MUB, MCB, and JSDM is 0.5, 3.8, 3.0, and 4.7 dB, respectively. They are not shown in the figure due to significant overlapping, which makes it hard to view them. Clearly BOON has a much smaller error bar than other schemes, i.e., has a more stable performance for different scenarios. On average, the SINR gain of BOON is about 8 dB over JSDM, and about 20 dB over MUB. MCB performs better than BOON on the UE SINR in the spread UE distribution pattern. However, this is at the expense of a lower sum rate, which can be seen from Fig. 7(a). This is because all UEs of a BS share one beam. Although the SINR is high, the spectral share per UE is small, and thus the sum rate is not high. On the other hand, BOON smartly adapts

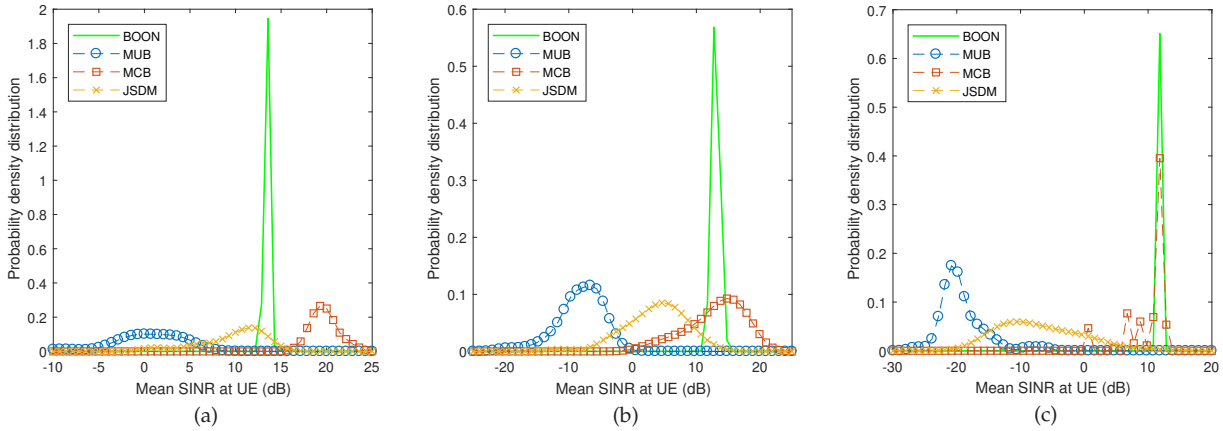

Fig. 10. Probability density distribution of mean SINR, (a) spread UE distribution, (b) grouped UE distribution, and (c) dense UE distribution, $\gamma_0 = 10$ dB.

to the UE distribution and determines the approximately optimal number of beams to be formed by each BS. Thus, even though the SINR is not as high as that of MCB, the spatial reuse of the spectral resource results in a higher sum rate for BOON compared with MCB.

The PDF of the mean SINR of all UEs for the 50 experiments is illustrated in Fig. 10, with $\gamma_o = 10$ dB. The PDF results of the mean SINR with different values of γ_o have similar trends and hence are omitted due to the space limitation. Similar to Fig. 8, overall the mean SINR of BOON has a much smaller deviation from the average value than other schemes. MCB has a higher SINR than BOON in the spread UE distribution pattern, but it has a lower sum rate. This is because MCB forms one beam per BS and avoids the inter-beam interference in a BS. Thus it achieves a high SINR. Nevertheless, the sum rate is the smallest as all UEs share the same beam, and thus the spectral share for each UE in a beam is small. MUB has the worst performance on SINR because forming one beam per UE causes excessive interference among beams.

Table 4 compares the computation complexity of BOON, MUB, MCB, and JSDM, where L is the number of elements of the BS antenna, $|\mathcal{U}|$ is the total number of UEs, $|B|$ is the number of BSs, k_i is the number of UEs for BS i in MUB, MCB and JSDM, G_i is the number of UE groups/beams for BS i in JSDM, q_i and Q_i are the number UEs and beams for BS i in BOON, respectively. Note that generally $q_i \neq k_i$ and $Q_i \neq G_i$ since the UE association and clustering of BOON and JSDM are different. The k_i is the same for MUB, MCB, and JSDM as they use the same user association scheme, the reference signal received power based UE association. The beamforming operation in (16–17) of Section 4.4 has to be conducted for every beam of each BS. Its time complexity is $\Theta(\max(kL^2, L^{2.373}))$, where k is the total number of UEs for a BS. For MCB, the time complexity is $\Theta(|\mathcal{U}|L^2)$ assuming the number of UEs for each BS is larger than $L^{0.373}$, which is $2.8, 3.6, 4.7$ when $L = 16, 32, 64$, respectively. For MUB, the time complexity is $\Theta(L^2 \sum_{1\leq i\leq |B|} k_i^2)$. For JSDM, the UE grouping based on channel covariance takes $\Theta(\sum_{1\leq i\leq |B|} k_i^2)$ time and the beamforming takes $\Theta(\sum_{1\leq i\leq |B|} k_i L^2 G_i)$ time. In general, $k_i < L^2 G_i$. Hence the time complexity of JSDM is $\Theta(L^2 \sum_{1\leq i\leq |B|} k_i G_i)$. For BOON, the UE clustering takes $\mathcal{O}(\sum_{1\leq i\leq |B|} q_i^2)$ time. The set covering by the IASC algorithm has a time complexity $\mathcal{O}(|\mathcal{U}||\mathcal{F}|)$. The time for CDSC is small and dominated by the set covering time. The beamforming takes $\Theta(\sum_{1\leq i\leq |B|} q_i L^2 Q_i)$ time. Again, generally $q_i < L^2 Q_i$. Moreover, the set covering time $\mathcal{O}(|\mathcal{U}||\mathcal{F}|)$ is typically smaller than $\Theta(\sum_{1\leq i\leq |B|} q_i L^2 Q_i)$. Hence the BOON time complexity is $\Theta(L^2 \sum_{1\leq i\leq |B|} q_i Q_i)$. From Table 4, in general the computation complexity of MCB is the lowest, while the one of MUB is the highest. The computation complexities of BOON and JSDM are comparable and both are between the ones of MCB and MUB.

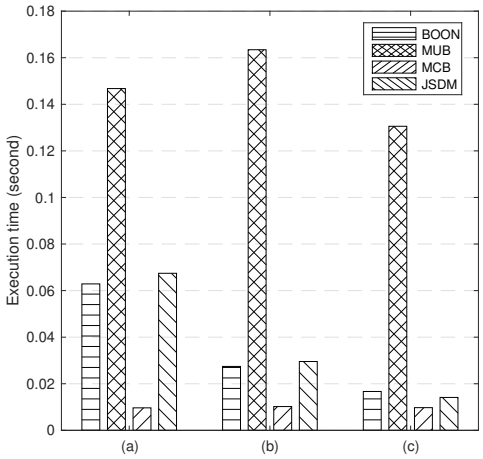

Fig. 11. Average execution time of the experiments in each UE distribution: (a) spread UE, (b) grouped UE , (c) dense UE.

Fig. 11 illustrates the average execution time of the experiments in each UE distribution, on a workstation with an Intel Core i7 CPU and 32 GB RAM. The execution time of BOON and JSDM are comparable and their time is between the ones of MCB and MUB. This is consistent with the time complexity comparison in Table 4. MUB uses much more time than BOON and JSDM in all scenarios. MCB uses less time than BOON and JSDM, but has much poorer performance on average.

TABLE 4
Computation complexity of BOON, MUB, MCB, and JSDM

	BOON	MUB	MCB	JSDM
Time complexity	$\Theta(L^2 \sum_{1 \le i \le \lvert B \rvert} q_i Q_i)$	$\Theta(L^2 \sum_{1 \le i \le \lvert B \rvert} k_i^2)$	$\Theta(L^2 \lvert \mathcal{U} \rvert)$	$\Theta(L^2 \sum_{1 \le i \le \lvert B \rvert} k_i G_i)$

6 Conclusion and Future Directions

We have developed a novel *Beamforming Oriented tOpology coNtrol* (BOON) framework for mmWave networks, with the objective to reduce the total transmit power of all BSs while forming beams to cover UEs. The BOON framework includes four components, UE clustering, set construction, set covering, and beamforming. We have compared BOON with the multi-user and multicast beamforming based topology control schemes, and a state-of-the-art scheme JSDM on transmit power, sum rate, SINR, and computation complexity. The results indicate that overall BOON significantly outperforms them. For instance, BOON uses only 10%, 32% and 25% transmit power on average, of the other three schemes, respectively, to achieve the same sum rate in the network.

For future directions, we will explore the possibility of incorporating NLOS paths in topology control. Moreover, we will study how to efficiently adjust the UE clustering, set covering, and beamforming to avoid re-running the entire process for a small number of UEs moving out of scopes of the original beams. Such improvements will strengthen BOON to efficiently address the UE mobility.

References

[1] Ericsson Report, "Internet of things forecast," 2018. [Online]. Available: https://www.ericsson.com/en/mobility-report/internet-of-things-forecast

[2] T. S. Rappaport, S. Sun, R. Mayzus, H. Zhao, Y. Azar, K. Wang, G. N. Wong, J. K. Schulz, M. Samimi, and F. Gutierrez, "Millimeter wave mobile communications for 5G cellular: It will work!" *IEEE Access*, vol. 1, pp. 335–349, May 2013.

[3] S. Rangan, T. S. Rappaport, and E. Erkip, "Millimeter-wave cellular wireless networks: Potentials and challenges," *Proc. of the IEEE*, vol. 102, no. 3, pp. 366–385, 2014.

[4] C. R. Anderson and T. S. Rappaport, "In-building wideband partition loss measurements at 2.5 and 60 GHz," *IEEE Transactions on Wireless Communications*, vol. 3, no. 3, pp. 922–928, 2004.

[5] F. Khan and Z. Pi, "mmWave mobile broadband (MMB): Unleashing the 3–300 GHz spectrum," in *Proc. IEEE Sarnoff Symposium*, 2011.

[6] Z. Pi and F. Khan, "An introduction to millimeter-wave mobile broadband systems," *IEEE Communications Magazine*, vol. 49, no. 6, pp. 101–107, 2011.

[7] J. G. Andrews, S. Buzzi, W. Choi, S. V. Hanly, A. Lozano, A. C. Soong, and J. C. Zhang, "What will 5G be?" *IEEE Journal on Selected Areas in Communications*, vol. 32, no. 6, pp. 1065–1082, 2014.

[8] B. Hu, C. Hua, C. Chen, X. Ma, and X. Guan, "MUBFP: Multiuser beamforming and partitioning for sum capacity maximization in MIMO systems," *IEEE Transactions on Vehicular Technology*, vol. 66, no. 1, pp. 233–245, 2017.

[9] D. Lee, G. Y. Li, X.-L. Zhu, and Y. Fu, "Multistream multiuser coordinated beamforming for cellular networks with multiple receive antennas," *IEEE Transactions on Vehicular Technology*, vol. 65, no. 5, pp. 3072–3085, 2016.

[10] L.-N. Tran, M. F. Hanif, and M. Juntti, "A conic quadratic programming approach to physical layer multicasting for large-scale antenna arrays," *IEEE Signal Processing Letters*, vol. 21, no. 1, pp. 114–117, 2014.

[11] J. Choi, "Iterative methods for physical-layer multicast beamforming," *IEEE Transactions on Wireless Communications*, vol. 14, no. 9, pp. 5185–5196, 2015.

[12] N. D. Sidiropoulos, T. N. Davidson, and Z.-Q. Luo, "Transmit beamforming for physical-layer multicasting," *IEEE Transactions on Signal Processing*, vol. 54, no. 6, pp. 2239–2251, 2006.

[13] A. Adhikary, E. Al Safadi, M. K. Samimi, R. Wang, G. Caire, T. S. Rappaport, and A. F. Molisch, "Joint spatial division and multiplexing for mm-wave channels," *IEEE Journal on Selected Areas in Communications*, vol. 32, no. 6, pp. 1239–1255, 2014.

[14] J. Yoon, K. Sundaresan, M. A. A. Khojastepour, S. Rangarajan, and S. Banerjee, "Joint multicell beamforming and client association in OFDMA small-cell networks," *IEEE Transactions on Mobile Computing*, vol. 15, no. 9, pp. 2260–2274, 2016.

[15] W.-L. Shen, K. C.-J. Lin, M.-S. Chen, and K. Tan, "SIEVE: Scalable user grouping for large MU-MIMO systems," in *Proc. IEEE Conference on Computer Communications (INFOCOM)*, 2015.

[16] X. Xia, S. Fang, G. Wu, and S. Li, "Joint user pairing and precoding in MU-MIMO broadcast channel with limited feedback," *IEEE Communications Letters*, vol. 14, no. 11, pp. 1032–1034, 2010.

[17] G. Dimic and N. D. Sidiropoulos, "On downlink beamforming with greedy user selection: performance analysis and a simple new algorithm," *IEEE Transactions on Signal processing*, vol. 53, no. 10, pp. 3857–3868, 2005.

[18] S. Huang, H. Yin, J. Wu, and V. C. Leung, "User selection for multiuser MIMO downlink with zero-forcing beamforming," *IEEE Transactions on Vehicular Technology*, vol. 62, no. 7, pp. 3084–3097, 2013.

[19] Z. Ding, P. Fan, and H. V. Poor, "Random beamforming in millimeter-wave NOMA networks," *IEEE access*, vol. 5, pp. 7667–7681, 2017.

[20] G. Lee, Y. Sung, and J. Seo, "Randomly-directional beamforming in millimeter-wave multiuser MISO downlink," *IEEE Transactions on Wireless Communications*, vol. 15, no. 2, pp. 1086–1100, 2016.

[21] C. N. Barati, S. A. Hosseini, S. Rangan, P. Liu, T. Korakis, S. S. Panwar, and T. S. Rappaport, "Directional cell discovery in millimeter wave cellular networks," *IEEE Transactions on Wireless Communications*, vol. 14, no. 12, pp. 6664–6678, 2015.

[22] Y. Li, J. G. Andrews, F. Baccelli, T. D. Novlan, and C. J. Zhang, "Design and analysis of initial access in millimeter wave cellular networks," *IEEE Transactions on Wireless Communications*, vol. 16, no. 10, pp. 6409–6425, 2017.

[23] H. Shokri-Ghadikolaei, C. Fischione, G. Fodor, P. Popovski, and M. Zorzi, "Millimeter wave cellular networks: A MAC layer perspective," *IEEE Transactions on Communications*, vol. 63, no. 10, pp. 3437–3458, 2015.

[24] M. R. Akdeniz, Y. Liu, M. K. Samimi, S. Sun, S. Rangan, T. S. Rappaport, and E. Erkip, "Millimeter wave channel modeling and cellular capacity evaluation," *IEEE journal on selected areas in communications*, vol. 32, no. 6, pp. 1164–1179, 2014.

[25] T. S. Rappaport, E. Ben-Dor, J. N. Murdock, and Y. Qiao, "38 GHz and 60 GHz angle-dependent propagation for cellular & peer-to-peer wireless communications," in *Proc. IEEE International Conference on Communications (ICC)*, 2012.

[26] Y. Cho and J. Kim, "Line-of-sight MIMO channel in millimeter-wave beamforming system: Modeling and prototype results," in *Proc. IEEE Vehicular Technology Conference*, 2015.

[27] M. Mahajan, P. Nimbhorkar, and K. Varadarajan, "The planar k-means problem is np-hard," *Theoretical Computer Science*, vol. 442, pp. 13 – 21, 2012.

[28] C. A. Balanis, *Antenna Theory: Analysis and Design, 3rd ed.* Wiley-Interscience, 2005.

[29] H. L. Van Trees, *Optimum array processing: Part IV of detection, estimation, and modulation theory*. John Wiley & Sons, 2004.

[30] E. Bjornson, M. Bengtsson, and B. Ottersten, "Optimal multiuser transmit beamforming: A difficult problem with a simple solution structure [lecture notes]," *IEEE Signal Processing Magazine*, vol. 31, no. 4, pp. 142–148, 2014.

[31] A. B. Gershman, N. D. Sidiropoulos, S. Shahbazpanahi, M. Bengtsson, and B. Ottersten, "Convex optimization-based beamforming," *IEEE Signal Processing Magazine*, vol. 27, no. 3, pp. 62–75, 2010.

Prosanta Paul received his B.S. in from Khulna University of Engineering and Technology, Bangladesh, in 2009, and M.S. in Electrical Engineering from South Dakota School of Mines and Technology, South Dakota, in 2014. He is currently pursuing his Ph.D. degree in the Department of Electrical and Computer Engineering, Old Dominion University. His research interests include cognitive radio networks, wireless communications, and networking.

Hongyi Wu is the Batten Chair of Cybersecurity and the Director of the Center for Cybersecurity Education and Research at Old Dominion University (ODU). He is also a Professor in Department of Electrical and Computer Engineering and holds joint appointment in Department of Computer Science. Before joining ODU, he was an Alfred and Helen Lamson Endowed Professor at the Center for Advanced Computer Studies (CACS), University of Louisiana at Lafayette (UL Lafayette). He received the B.S. degree in scientific instruments from Zhejiang University, Hangzhou, China, in 1996, and the M.S. degree in electrical engineering and Ph.D. degree in computer science from the State University of New York (SUNY) at Buffalo in 2000 and 2002, respectively. His research focuses on networked cyber-physical systems for security, safety, and emergency management applications, where the devices are often light-weight, with extremely limited computing power, storage space, communication bandwidth, and battery supply. He received NSF CAREER Award in 2004 and UL Lafayette Distinguished Professor Award in 2011.

ChunSheng Xin is a Professor in the Department of Electrical and Computer Engineering, Old Dominion University. He received his Ph.D. in Computer Science and Engineering from the State University of New York at Buffalo in 2002. His interests include cybersecurity, wireless communications and networking, cyber-physical systems, and Internet of Things. His research has been supported by almost 20 NSF and other federal grants, and results in more than 100 papers in leading journals and conferences, including three Best Paper Awards, as well as books, book chapters, and patent. He has served as Co-Editor-in-Chief/Associate Editors of multiple international journals, and symposium/track chairs of multiple international conferences including IEEE Globecom and ICCCN. He is a senior member of IEEE.

Min Song (F'18) is currently Professor and Chair of the department of electrical and computer engineering at Stevens Institute of Technology. Before joining Stevens, he was the David House Professor and Chair of the computer science department and Professor of electrical and computer engineering at Michigan Tech from 2014 to 2018. He was also the Founding Director of the Michigan Tech Institute of Computing and Cybersystems. Prior to joining Michigan Tech, Min served as Program Director with the National Science Foundation (NSF) from 2010 to 2014. Min's current research interests are in the areas of cognitive radio networks, Internet of Things, energy harvesting, artificial intelligence, and wireless communication networks. Over the course of his career, Min has published more than 160 technical papers and held various leadership positions. He also served as the IEEE Communications Society director of conference operations, member of the board of governors (2016-2017) and as journal editor and conference chair on several initiatives. Min was the recipient of NSF CAREER award in 2007. He is an IEEE Fellow.